Submitted to Astrophysical Journal: April 11, 2012

Scaler mode of the Auger Observatory and Sunspots

Carlos A. García Canal

Instituto de Física La Plata, CCT La Plata, CONICET and
Departamento de Física, Facultad de Ciencias Exactas,
Universidad Nacional de La Plata
CC 67, 1900 La Plata, Argentina

Carlos Hojvat

Fermilab, P.O. Box 500 – Batavia IL 60510-0500, USA.

Tatiana Tarutina

Instituto de Física La Plata, CCT La Plata, CONICET and
Departamento de Física, Facultad de Ciencias Exactas,
Universidad Nacional de La Plata
CC 67, 1900 La Plata, Argentina

Abstract

Recent data from the Auger Observatory on low energy secondary cosmic ray particles are analyzed to study temporal correlations together with data on the daily sunspot numbers and neutron monitor data. Standard spectral analysis demonstrates that the available data shows $1/f^{\beta}$ fluctuations with $\beta \approx 1$ in the low frequency range. All data behave like Brownian fluctuations in the high frequency range. The existence of long-range correlations in the data was confirmed by detrended fluctuation analysis. The real data confirmed the correlation between the Hurst exponent of the detrended analysis and the exponent of the spectral analysis.

Subject headings: Auger scalers, sunspots, 1/f fluctuations, Hurst exponent

1. Introduction

Solar activity gives rise to a modulation of the flux of cosmic rays observed at Earth. The Pierre Auger Observatory (Pierre Auger Observatory) has made available the scaler singles rates observed on their surface detectors reflecting the counting rates of low energy secondary cosmic ray particles (Pierre Auger Collaboration 2008, 2011). These data are presented after corrections for atmospheric effects, pressure in particular, and compared with temporal variations of solar activity as shown by data obtained with neutron monitors (Neutron Monitor Database 2011). Solar and cosmic rays data can be presented as a temporal series containing modulations, correlations and noise fluctuations. The availability of Auger scaler data and data from neutron monitors and sunspot numbers (SIDC 2011) motivated us to study the existence of long-range correlations present in the corresponding time series.

The low threshold rates or scaler data have been recorded by the surface detectors of Auger Observatory since March 2005. These data should be sensitive to transient events such as Gamma Ray Bursts and solar flares. The rates at each detector are registered every second and the 15 minute average rates are available for public use (Auger Scalers online 2011). The temporal variations can be accurately studied, as these rates are very large as compared to other data on solar activity.

In the work of Pierre Auger Collaboration (2011) the pressure corrected Auger scalers were compared to data from the Rome neutron monitor (Storini et al.) and it was concluded that Auger scalers could be suitable for the study of solar activity.

A sunspot is a temporary phenomenon in the solar photosphere that appears like a dark visible spot compared to the surrounding regions (see, for example, Bray & Loughhead (1979)). It corresponds to a relatively cool area of the Sun photosphere (1500 K less than the average photosphere temperature) as a result of the heat convection process inhibition by intense magnetic fields.

The number of sunspots and their position on the Sun face change with time as a consequence of the solar activity cycle. The maximum solar activity corresponds to a large number of sunspots and in the minimum less sunspots are observed. The spots usually appear in groups.

Data on sunspots are available for the last four centuries. From 1749 to 1981 the sunspot data were provided by the Zürich Observatory. Nowadays the Solar Influences Data Analysis Center (SIDC 2011) is responsible for recording sunspot data.

Neutron monitors are ground based detectors that measure the flux of cosmic rays from the Sun and low-energy cosmic rays from elsewhere in the Universe. In a typical neutron monitor, low-energy neutrons produced by nuclear reactions in lead are slowed down to thermal energies by a moderator and detected by proportional counter tubes. A worldwide network consisting of approximately 50 stations is in operation and their data are available on-line (Neutron Monitor Database 2011).

For this analysis we select data from two neutron monitoring stations. Those sites were chosen by the availability of complete data for all the days of the period of availability of Auger scaler data. Therefore there was no necessity to perform an interpolation procedure. These 2 neutron monitor are known as JUNG ((JUNG)) and APTY ((APTY)). The JUNG detector is located on top of the Sphinx Observatory Jungfraujoch, Switzerland and APTY is situated in the town of Apatity, Russia.

The aim of this note is to present a systematic analysis of the temporal series from different experimental determinations. This analysis, based on power spectra behavior (Fanchiotti et al. 2004) and detrended power behavior (Fanchiotti et al. 2004; Peng et al. 1994) allows us to gain quantitative information about correlations among the different phenomena. It is also interesting to study the connection between the information provided by the power spectra analysis and the detrended analysis for the case of real data.

This paper is organized as follows: in section 2 we present the results of the power spectra analysis of the three data sets and in section 3 we present the results of the corresponding detrended analysis. In section 4 final remarks are given.

2. Power Spectra

There is a number of accepted techniques (Hamilton 1994) to characterize random processes $x(t)$. Usually one starts with the correlation function defined as

$$G(\tau) = \langle x(t_0)x(t_0+\tau)\rangle_{t_0} - \langle x(t_0)\rangle^2_{t_0}. \tag{1}$$

Another widely used tool is the frequency spectrum that is defined as the squared amplitude of the Fourier transform of the time signal:

$$S(f) = \lim_{T\to\infty} \frac{1}{T} \left| \int_{-T}^{T} d\tau x(t) e^{2i\pi f\tau} \right|^2 . \tag{2}$$

For a stationary process, the frequency spectrum is connected with the temporal correlation function through the Wiener-Khintchine relation (MacDonald 1962):

$$S(f) = 2\int_0^\infty d\tau G(\tau)\cos(2\pi f\tau). \tag{3}$$

A true random process, also called white noise has no correlations in time, therefore the correlation function for the white noise is zero and the spectrum function $S(f) \propto$ const. The integral of white noise over time produces Brownian motion (MacDonald 1962) or random walk with the spectrum function $S(f) \propto 1/f^2$.

Many naturally occurring fluctuations of physical, biological, economic, traffic and musical quantities exhibit $S(f) \propto 1/f$ behavior over all measured time scales (see, for example, Voss & Clarke (1975); Press (1978); Van Vliet (1991); Baillie (1996); Novikov et al. (1997)). These fluctuations are of interest because they correspond to the existence of extremely long-range time correlations in the time signals. This can be shown (see Jensen (1998)) if one assumes that the spectral function of a time signal $S(f) \propto 1/f^\beta$ and that the temporal correlation function $G(\tau) \propto$

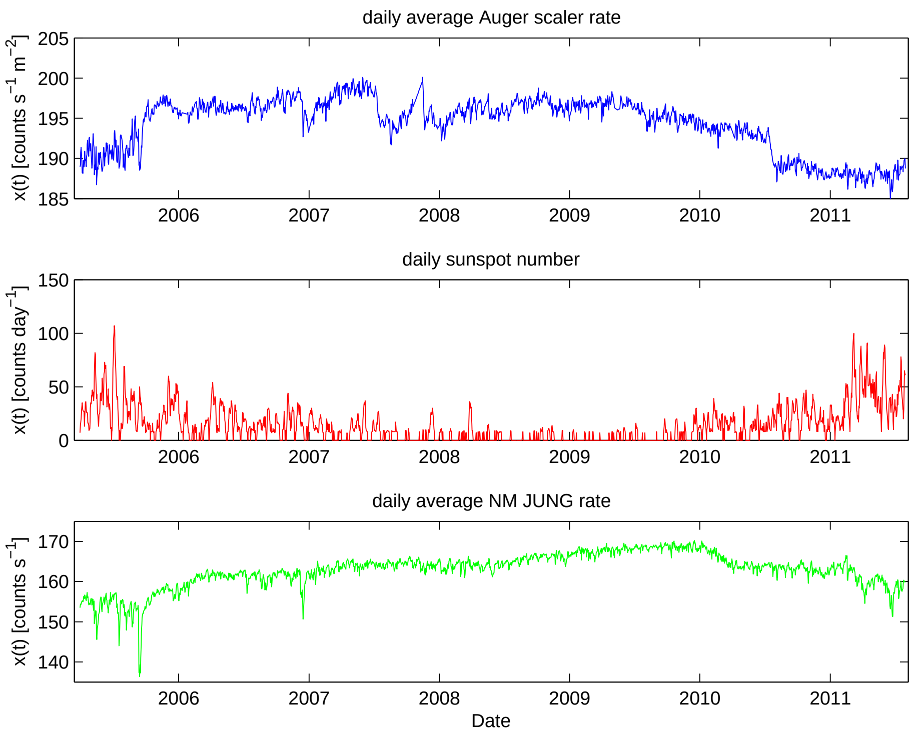

Fig. 1.— (Color online) Auger scalers, Sun spots and neutron monitor JUNG data.

$1/\tau^{\alpha}$. It follows from (3) that $1/f^{\beta} \propto 1/\tau^{1-\alpha}$. When $\beta \approx 1$ it follows that $\alpha \approx 0$ which corresponds to correlation function $G(\tau) \approx 1$.

An analysis of monthly sunspot data was performed in the work of Fanchiotti et al. (2004), including the study of the power spectra and detrended analysis. It was found that the high frequency part of the spectral function of the monthly sunspots shows the $1/f^{\beta}$ behavior with $\beta = 0.8 \pm 0.2$. This corresponds to the $1/f$ noise.

In Figure 1 we present the available time series data: (1) Auger scalers, (2) sunspots and (3) JUNG neutron monitor data for the time period when data on the Auger scalers are available. As the Auger scalers contained gaps, sometimes of various days, in order to use it in the analysis we performed an interpolation of the data justified by the Brownian behavior of data for the high frequencies.

In Figure 2 we present the power spectra of available data on a logarithmic scale vs. frequency. The power spectra for the sunspots and the neutron monitor were shifted with respect to each other to avoid overlap. The spectral function indicates the presence of two different behaviors for low and high frequencies that can be approximated by linear function with the smaller slope in the range of lower frequencies. The frequency corresponding to the change from one region to another is different for each data set. We also note that in the sunspot daily spectra there is a peak corresponding to the frequency of approximately 1/27=0.04 days^{-1} ($\log(f) \approx -1.4$), not clearly seen on Figure 2 because of the low statistics. This 27-day peak is due to solar rotation (Bray & Loughhead 1979). At first sight the description with the piecewise linear function seems more justified for the spectral function of the sunspots than in the spectral function of the scalers which shows more attenuated behavior for relatively small frequencies. In addition, the slope for the low frequency part of the spectrum for the Auger scalers and the neutron monitor is smaller compared with that of the sunspots. We make a further analysis of these facts below.

We analyzed the power spectra of Auger scalers, sunspots and two neutron monitors using a linear least squares fit. First we fitted the data for the total range of frequencies. The resulting β is presented in the second column of Table 1. All data have similar slopes when fitted over the total range of the frequencies giving $\beta \approx 1.6$.

Second, we performed a fit of the data to the piecewise linear function consisting of two parts with different slopes. The frequency corresponding to the point of change of the slope f_c was adjusted independently for each data set to obtain the best fit. The results are presented in Table 2 and in Figure 3. It is seen from this analysis that in the low frequency range all data show the existence of long-range correlations with $\beta \approx 1$. For high frequencies, the spectral function shows the Brownian behavior. It is also seen that the position of f_c is different for each the data set. It should be noted that in the case of sunspots the position of f_c could be dictated by the existence of 27-day cycle of the Solar activity (Bray & Loughhead 1979).

In order to have more quantitative conclusions about the value of β for the data we performed a systematic fit of all data for different frequency ranges. In Figure 4(a) we show the fitted slope β

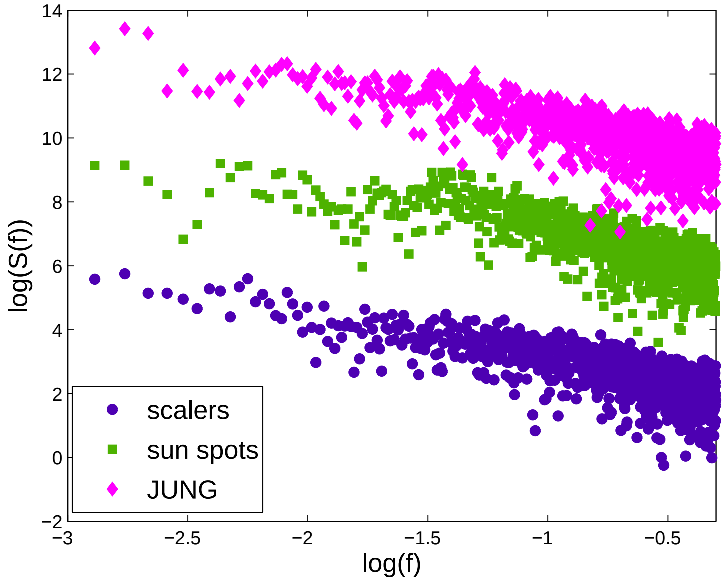

Fig. 2.— (Color online) Power spectra of daily Auger scalers, sunspots, and the neutron monitor JUNG.

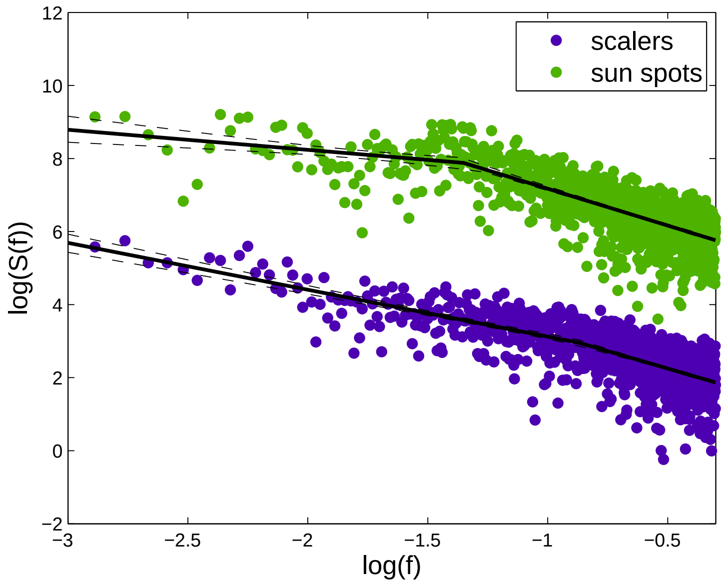

Fig. 3.— (Color online) Power spectra of daily Auger scalers and sunspots with the corresponding result of the fit with piecewise linear function (solid lines). Dashed lines indicate 95% prediction bounds.

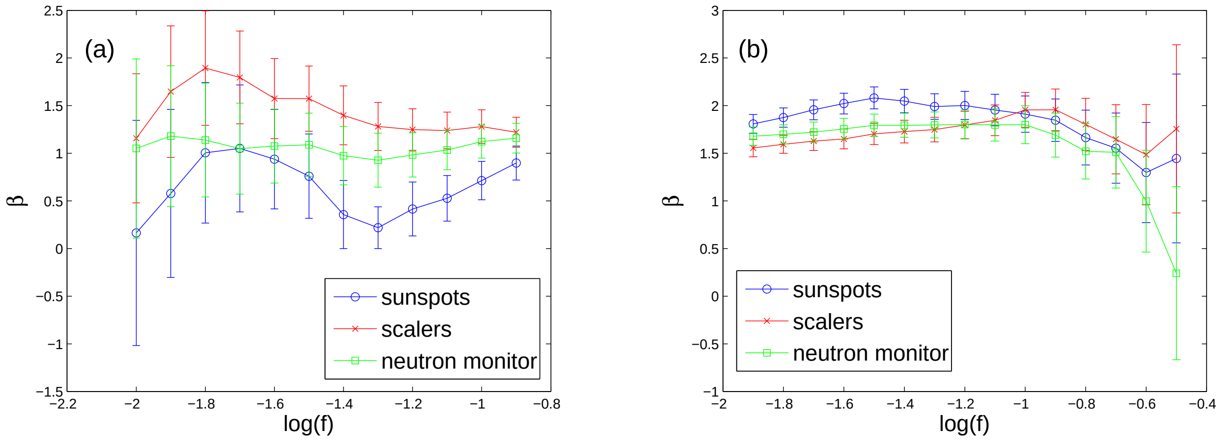

Fig. 4.— The dependence of the power spectra slope β on the range of the frequency used for the fit: (a) low frequency range; (b) high frequency range. See text for explanation.

for sunspots, Auger scalers and neutron monitor JUNG obtained on the interval of low frequencies. In this analysis we set the lowest frequency to be $\log(f) = -3$ (in order to remove the outliers) and vary the size of the interval taking into account the power spectra up to certain value of $\log(f)$. That is, the point with smaller $|\log(f)|$ in Figure 4(a) corresponds to the larger frequency range used for fitting. For the range of frequencies $-3.0 < \log(f) < -1.0$ the data on sunspots, Auger scalers and neutron monitor show $\beta \approx 1$. In the case of sunspots for $\log(f) < -1$ the drop in β can be explained by the influence of the mentioned 27-day peak which is not seen in the case of Auger scalers and neutron monitors. For larger values of $|\log(f)|$ the error is large for all the data because of the low statistics but the results agree within the error bars.

In Figure 4(b) we show the results of a similar analysis but for the high frequency range. Here we obtain the value of β fitting the data over the frequency interval with varying size starting from some value of $\log(f)$ and up to $\log(f) = \log(f_N)$, where f_N stands for the Nyquist frequency. That is, the point with larger value of $|\log(f)|$ in Figure 4(b) corresponds to the larger frequency range used for fitting. It is seen that for $\log(f) \approx -1$ all the data predict a similar value of β. For smaller values of $\log(f)$ the value of β drops because of the influence of the part of the frequency spectra corresponding to $\beta \approx 1$.

Finally, we divide the range of frequencies into two regions: (a) a low frequency region $\log(f) \lesssim -1$ and (b) a high frequencies region $\log(f) \gtrsim -1$; fitting the data to a linear dependence in each region. The results of the linear fit are shown in the third and forth columns of the Table 1.

For the high frequency range, the data show agreement with the following behavior:

$$S(f) \approx f^{-1.9\pm0.2} \tag{4}$$

which corresponds to Brownian fluctuations. This is an expected behavior because at high frequencies the fluctuations become more random, that is with less correlations.

We can conclude that the data show the coexistence of two behaviors in the power spectra: (1) consistent with a $1/f$ dependence for low frequencies (2) consistent with a $1/f^2$ behavior for high frequencies. Our analysis confirms the result of Fanchiotti et al. (2004) where monthly data on the sunspots was analyzed. The sunspots in this frequency region have $1/f$ behavior. The $1/f^2$ behavior was not detected in Fanchiotti et al. (2004) because it corresponds to the high frequencies which are not present in monthly data.

3. Detrended fluctuation analysis

Another statistical method to reveal the extent of long-range temporal correlations in time series is the Detrended Fluctuation Analysis (DFA). This method was introduced in Peng et al. (1994) and applied in many areas of research, including physical and biological sciences.

Consider the time series $x(t)$ consisting of N samples. The procedure is as follows:

1. First generate a new time series $u(t_n)$ by means of:

$$u(t_n) = \sum_{k=1}^{n} x(t_k), \;\; u(0) = 0, \;\; n = 1, \ldots, N. \tag{5}$$

2. Divide the time series $u(t)$ into non-overlapping intervals of equal length s. In each interval the data is fitted using least-squares to the first order polynomial (the polynomial of 2nd, 3d order may be used as well, see Kantelhardt et al. (2002)), giving a local trend $y(t) = at + b$.

3. In each interval calculate the detrended fluctuation function using:

$$[F(s)]^2 = \sum_{t=ks+1}^{(k+1)s} [x(t) - y(t)]^2; \;\;\; k = 0, 1, \cdots, (\frac{N}{s} - 1)$$

4. Calculate the average of $F(s)$ over N/s intervals.

data set	total range slope	high frequency slope	low frequency slope
Auger scalers	-1.525 ± 0.073	-1.96 ± 0.18	-1.38 ± 0.16
Sun spots	-1.591 ± 0.080	-1.91 ± 0.19	-0.81 ± 0.19
NM JUNG	-1.564 ± 0.078	-1.80 ± 0.20	-1.22 ± 0.16
NM APTY	-1.549 ± 0.079	-1.97 ± 0.20	-1.22 ± 0.19

Table 1: Slopes of the linear least squares fitting model for different frequency ranges.

For a fluctuating time series, the expected behavior is as follows:

$$\langle F(s) \rangle \sim s^{H_\alpha}$$

where H_α is the Hurst exponent. The situation when $H_\alpha = 1/2$ corresponds to random walk. The long-range correlations reveal themselves through the $H_\alpha \neq 1/2$.

Initially the detrended fluctuation analysis was proposed as an independent measure of long-term correlation, complementary to the spectral analysis information. In the work of Buldyrev (1995) it was noted that the value of β of the spectral function and $\beta' = 2H_\alpha - 1$ are 'remarkably close to each other'. Heneghan & McDarby (2000) examined the analytical link between DFA and spectral analysis and showed that they are related through an integral transform. It was concluded that DFA and spectral measures provide equivalent characterizations of stochastic signals with long-term correlation. In this work we study the connection between the Hurst coefficient H_α and the coefficient β introduced in the spectral function analysis partially to check this assertion in this particular case with the real data.

In Figure 5 the result of the detrended fluctuation analysis of Auger scalers, sunspot numbers and one neutron monitor (JUNG) is shown. In the case of the sunspots, the data can be separated into 3 regions with different slopes: (a) $\log(s) \lesssim x$; (b) $x \lesssim \log(s) \lesssim 2.0$ and $\log(s) \gtrsim 2.0$ (the numbers here are approximate). The value of $x = 1.3$ approximately corresponds to the 27-day peak in the spectral function of the daily sunspots. For the case of Auger scalers and neutron monitors the existence of three regions in the DFA curve is not as clear as in the case of the sunspots but a close examination of Figure 5 suggests a change of slope at $\log(s) \approx 1$ for Auger scalers and neutron monitors. The situation is similar to the power spectra curves where the difference between the regions with $1/f$ and $1/f^2$ is more apparent for the case of the sunspots. There is a correspondence between the frequency in the power spectra of the time series and the value of s. The region of large values of $\log(s)$ corresponds to the very small frequencies of the time series and have large fluctuations that can be seen on the Figure 5. This region of large values of $\log(s)$ is excluded from our analysis.

In Table 3 we compare the exponent β, and $\frac{\beta+1}{2}$, with the coefficient H_α which characterized the slope obtained in the DFA analysis for two ranges of the frequencies: (a) 'high frequency' $\log(s) \lesssim x$ and (b) 'low frequency' $x \lesssim \log(s) \lesssim 2.0$, where x is taken equal to the logarithm of the frequency corresponding to the change of the regimen in the power spectra (and given in Table 2). First of all it is seen that the calculated Hurst exponent for low frequencies is always

quantity	Auger scalers	Sunspots	NM JUNG	NM APTY
$\log(f_c)$	-0.87	-1.35	-1.25	-1.15
β low	-1.28 ± 0.14	-0.55 ± 0.32	-1.12 ± 0.23	-1.11 ± 0.22
β high	-1.91 ± 0.23	-2.02 ± 0.13	-1.79 ± 0.14	-1.86 ± 0.16

Table 2: Slopes of the linear least squares fitting model for different frequency ranges.

$H_\alpha > 1/2$ which implies the existence of long-range correlations. It should be noted that the analysis of the daily sunspot numbers confirmed the result of the analysis of the monthly sunspot number performed by Fanchiotti et al. (2004), where the value obtained for the Hurst exponent was $H_\alpha = 0.62 \pm 0.4$. It corresponds to the low frequencies as the high frequencies are not seen in the monthly data.

In order to compare the results of power spectra analysis and DFA we present in Figure 6 the slopes calculated using these two methods with the error bars indicated. The results are grouped by frequency: to the left for low frequencies and to the right for high frequencies. In each of these groups we present the resulting $\frac{\beta+1}{2}$ from spectral analysis (filled markers) and the Hurst exponent from DFA (open markers). It is seen that the results of both methods agree within the error bars and are consistent with $H_\alpha \approx 1$ for low frequencies and $H_\alpha \approx 3/2$ for high frequencies. Thus, in this work using real data of three different sources we confirm the correspondence between the value of β of the spectral function and Hurst exponent of detrended fluctuation analysis for both frequency ranges.

4. Final remarks

We have presented a statistical study of the available data on Auger scalers, sunspots and neutron monitors. We studied the frequency spectra and performed a detrended analysis. We found that the spectral function can be separated into two regions: (1) the region of the low frequencies and (2) the region of high frequencies that can be described by power laws. It was shown that the low-frequency part of the spectral function of all data shows $1/f$ behavior. Because of the low statistics the error is large. The high frequency part of the spectral function of all data is shown to behave like Brownian fluctuations. This similar behavior of the time series analyzed can be understood because all three kinds of events are correlated since they have their origin in the solar activity.

The detrended analysis performed confirmed the existence of long-range correlations, for low frequencies, in all available data (the Hurst coefficient $H_\alpha \gtrsim 1$). Finally, the correspondence between the Hurst exponent and the β exponent of the spectral analysis was confirmed with real data.

5. Acknowledgements

We would like to warmly thank Professors Huner Fanchiotti and Sergio Sciutto for very useful discussions. We acknowledge the Pierre Auger Observatory for making the data publicly available and the Pierre Auger Collaboration Publication Committee for a critical reading of the text. Fermilab is operated by Fermi Research Alliance, LLC under Contract No. De-AC02-07CH11359 with the United States Department of Energy. CAGC y TT acnowledge partial support of ANPCyT of

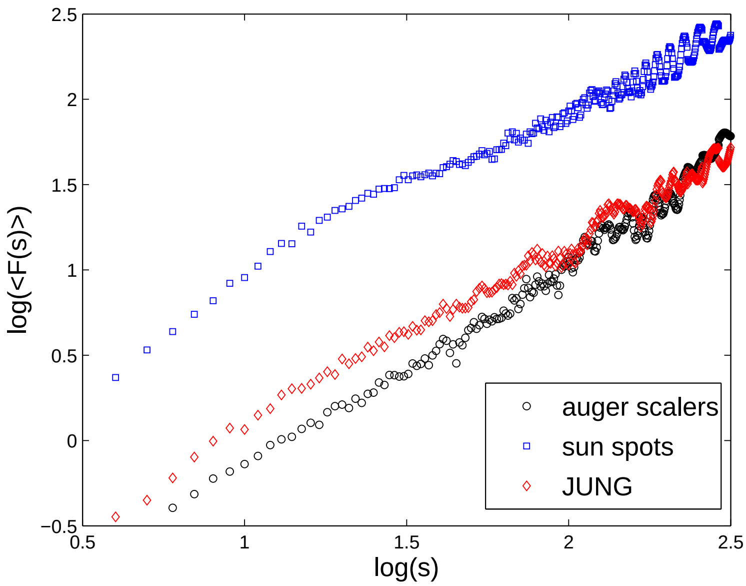

Fig. 5.— (Color online)Detrended fluctuation analysis curves of Auger scalers, sunspots and neutron monitor JUNG.

frequency	β	$\frac{\beta+1}{2}$	H_α
Sunspots			
high	2.02 ± 0.13	1.51 ± 0.08	1.40 ± 0.06
low	0.55 ± 0.32	0.78 ± 0.16	0.75 ± 0.03
Auger scalers			
high	1.91 ± 0.23	1.46 ± 0.12	1.39 ± 0.16
low	1.28 ± 0.14	1.14 ± 0.07	1.14 ± 0.03
NM JUNG			
high	1.79 ± 0.14	1.40 ± 0.07	1.33 ± 0.09
low	1.12 ± 0.23	1.06 ± 0.12	0.96 ± 0.04
NM APTY			
high	1.86 ± 0.16	1.43 ± 0.08	1.38 ± 0.11
low	1.11 ± 0.22	1.06 ± 0.06	0.97 ± 0.03

Table 3: The result of the spectra analysis $\frac{\beta+1}{2}$ and Hurst exponent H_α from DFA for sunspots, Auger scalers and two neutron monitors.

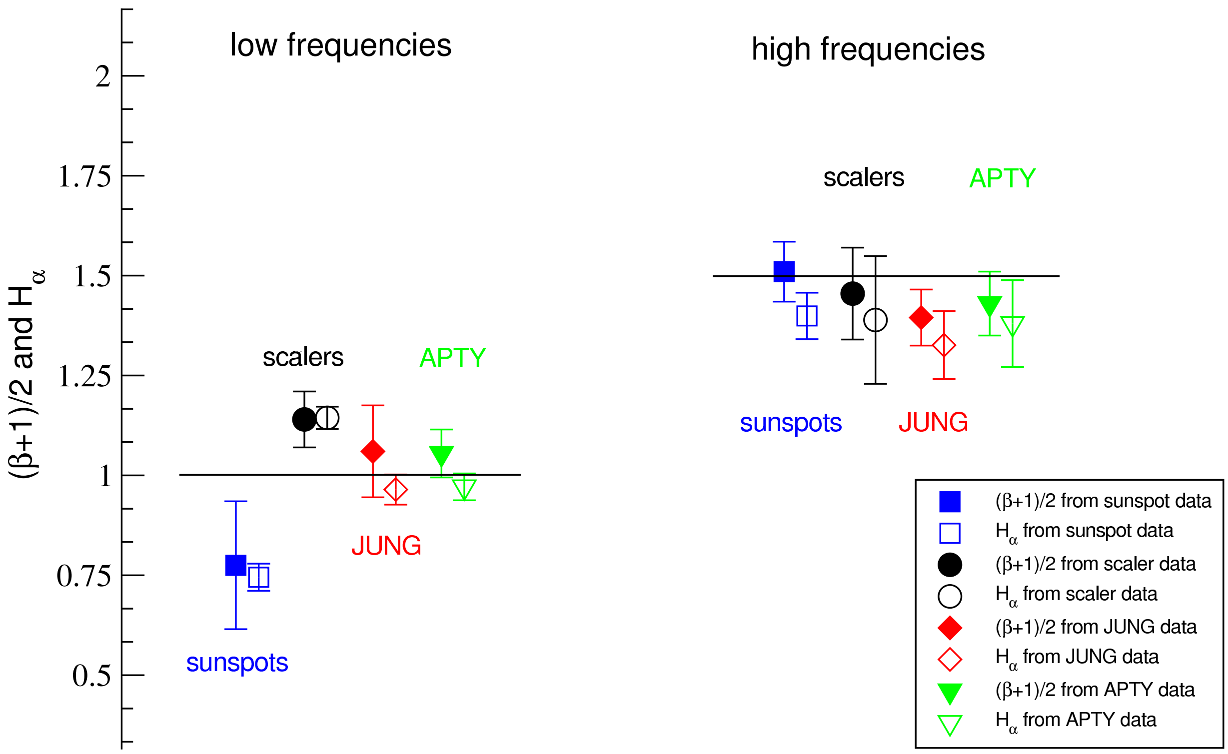

Fig. 6.— (Color online) Comparison between $\frac{\beta+1}{2}$ and Hurst exponent for sunspot, Auger scaler and neutron monitor data calculated in the regions of high and low frequencies.

Argentina.

REFERENCES

Pierre Auger Observatory, http://www.auger.org

Pierre Auger Collaboration, Bertou X. 2008, in Proceedings of the 30th International Cosmic Ray Conference (ICRC 2007)(Mexico DF, Mexico), pg.441-444

Pierre Auger Observatory Collaboration 2011, JINST, 6, P01003

Neutron Monitor Database, http://www.nmdb.eu/nest/search.php

Solar Influences Data Analysis Center, http://sidc.oma.be/sunspot-data/

Auger Scaler data online, http://auger.colostate.edu/ED/scaler.php

M. Storini et al., Rome Neutron Monitor, supported by INAF/UNIRomaTre collaboration, http://cr0.izmiran.rssi.ru/rome/main.htm

Bray, R.J., Loughhead, R.E. 1979, Sunspots, (Dover Publications, New York)

Neutron monitor JUNG, http://www.nmdb.eu/?q=node/12

Neutron monitor APTY, http://www.nmdb.eu/?q=node/118#Apatity

Fanchiotti, H., Sciutto, S. J., García Canal, C.A., and Hojvat, H. 2004, Fractals, 4, 405

Peng, C.K., et al. 1994, Phys. Rev. E, 49, 1685

Hamilton, J. 1994, Time Series Analysis, (Princeton: Princeton Univ. Press)

MacDonald, D.K.C. 1962 ,Noise and Fluctuations: An Introduction, (New York: Wiley)

Voss R.F., and Clarke, J. 1975, Nature, 258, 317

Press, W.H. 1978, Comments Astrophys., 7, 103

Van Vliet, C.M. 1991, Solid-State Electron., 34, 1

Baillie, R.T. 1996, J. Economet., 73, 5

Novikov, E., Novikov, A., Shannahoff-Khalsa, D., Schwartz B., and Wright, J. 1997, Phys. Rev. E, 56, R2387

Jensen, H.J. 1998, Self-Organized Criticality, (Cambridge University Press)

Kantelhardt, J.W., Zschiegner, S.A., Koscielny-Bunde, E., Havlin, S., Bunde, A., and Stanley, H.E. 2002, Physica A, 316, 87

Buldyrev, S.V. 1995, *et al.*, Phys. Rev. E, 51, 5084

Heneghan, C., and McDarby, G. 2000, Phys. Rev. E, 62, 6103